Chapter – VI

Theoretical Study of the Effect of Surface Roughness on the Static Characteristics of Inclined Plane Slider Bearing: Rabinowitsch Fluid Model

6.1 Introduction

The study of slider bearings has attracted the attention of several researchers in recent years as these are amenable to easy mathematical analysis. Slider bearings are often encountered in engineering applications. They support or guide the parts movably opposed to each other as well as absorb and transfer the occurring forces. Such bearings are used for supporting transverse loads. Slider bearings have been studied for various film shapes, Pinkus and Sternlitchi (1961), Hamrock (1994), Bagci and Singh (1983). It is well known that, due to run-in and wear causes roughness in bearing surfaces. Contamination of lubricant is also responsible for making the bearing surface rough through chemical degradation. The random character of surface roughness was recognized by several investigators who used a stochastic approach to mathematically model the roughness of the bearing surfaces Tzeng and Saibel (1967), Christensen and Tonder (1969a, 1969b) further developed this approach and proposed a comprehensive general analysis both for transverse and longitudinal surface roughness based on a general probability density function. Applying the concept of a stochastic process, a modified Reynolds equation for rough bearing surfaces is derived by Christensen (1969-70). It is observed that, surface roughness may considerably influence the bearing characteristics. Many researchers have studied different types of bearings with roughness effect such as the investigations in the hydrostatic bearing by Lin (2000), the journal bearing by Turaga *et al.* (1999), Guha (2000) and the slider bearing by Christensen and Tonder (1971). Recently, Naduvinamani *et..al.* (2007) analyzed combined effects of surface roughness and couple stresses on squeeze film lubrication between porous circular stepped plates. This theory has been widely used to investigate the effects of couple stresses on the performance of different

type of fluid film bearings such as slider bearings (2005, 1979) journal bearings (2002, 2001).

In the Rabinowitsch fluid model, the following empirical stress strain relation is as given in equation (2.1.1). Recently, several researchers have investigated the non-Newtonian effect of Rabinowitsch lubricants on various types of bearings. Lin *et.al* (2001), studied the non-Newtonian effect of Rabinowitsch fluid model on the slider bearings, parallel annular disks by Lin, (2012) and parallel rectangular squeeze film plates by Lin *et al*. (2013). Squeeze film characteristics between a long cylinder and a flat plate by Singh *et.al.* (2013), non-Newtonian effects on the squeeze film characteristics between a sphere and a flat plate: Rabinowitsch Fluid model studied by Singh and Gupta (2012).

In this chapter, we seek to study the effect of surface roughness on the performance of one dimensional slider bearings lubricated with Rabinowitsch fluid, which has not been studied so for.

6.2 Mathematical formulation of the problem

The Physical geometry of inclined rough plane slider bearing of length L is shown in Figure 6.1. The lubricant in the film region is considered to be Rabinowitsch fluid. The sliding velocity of lower bearing surface is U in the x-direction. The body forces and body couples are assumed to be absent. For the present problem the film thickness can be described by

$$h(x,y)=(h_1-h_2).(1-x/L)+h_2. \tag{6.2.1}$$

Under the usual assumptions of hydrodynamic lubrication theory, equations of continuity and motion in cartesian coordinates reduces to

$$\frac{\partial u}{\partial x}+\frac{\partial v}{\partial y}=0, \tag{6.2.2}$$

$$\frac{\partial p}{\partial x}+\frac{\partial \tau_{xy}}{\partial y}=0, \tag{6.2.3}$$

$$\frac{\partial p}{\partial x}=0. \tag{6.2.4}$$

The relevant boundary conditions for velocity components are

i. At the upper surface $y = H$

$$u = 0 \quad \text{and} \quad v = 0; \tag{6.2.5a}$$

ii. At the lower surface $y = 0$

$$u = U \quad \text{and} \quad v = 0. \tag{6.2.5b}$$

Let the local film thickness H can be considered to be composed of two separate parts

$$H = h(x,y) + h_s(x,y,\xi) \tag{6.2.6}$$

where $h(x, y)$ denotes the nominal smooth part of the film geometry while h_s the part due to the surface roughness is measured from the nominal level. Without loss of generality it may be assumed that, the mean value of h_s over bearing surface is zero. The film thickness component h_s is the function of space co-ordinates x and y, and of the random variable ξ. Hence, for a given value of ξ the surface component of the film thickness becomes deterministic function of the space variables.

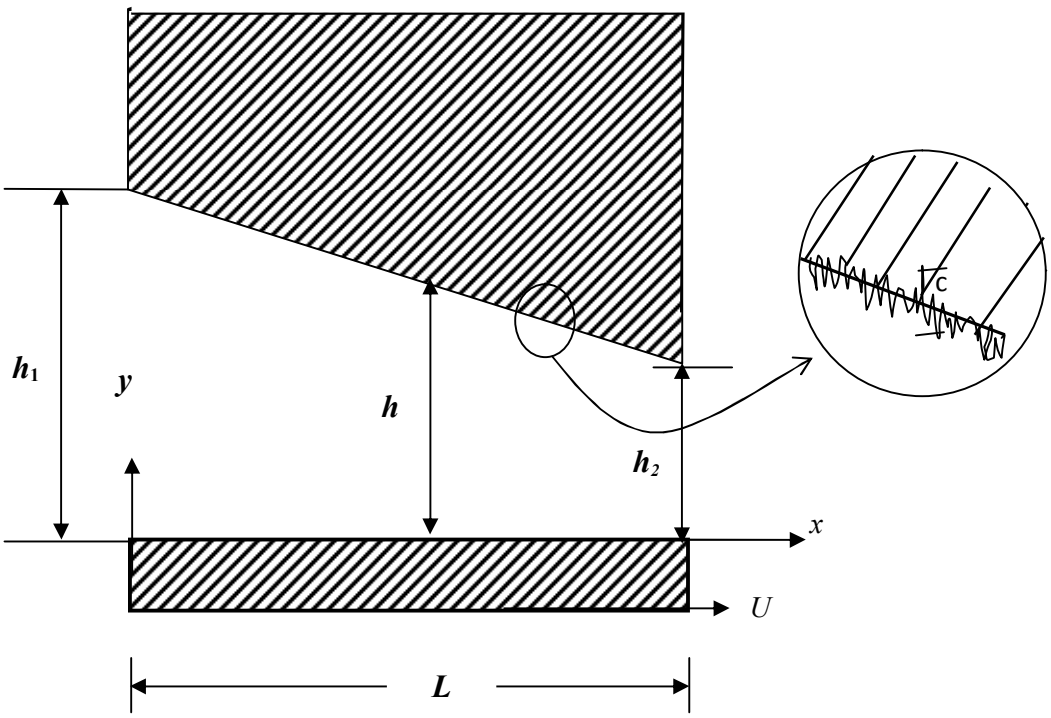

Figure 6.1 Physical geometry of inclined rough plane slider bearing

6.3 Solution of the problem

Integrating equation (6.2.3) with respect to y and using boundary conditions (6.2.5a) and (6.2.5b) and using equation (2.1.1) the expression for velocity component in x-direction is given by

$$u = \frac{1}{4\mu}\left[2\left(\frac{\partial p}{\partial x}\right) y^2 + 4c_1 y + \alpha\left\{ \left(\frac{\partial p}{\partial x}\right)^3 y^4 + 4\left(\frac{\partial p}{\partial x}\right)^2 c_1 y + 6\left(\frac{\partial p}{\partial x}\right) c_1^2 y^2 + 4c_1^3 y \right\}\right] + c_2 \tag{6.3.1}$$

Integration constants c_1 and c_2 can be determined by using the boundary conditions (6.2.5a) and (6.2.5b) and simplifying further, the velocity component u in x- direction can be obtained as

$$u = \frac{1}{4\mu}\left[F_1 \frac{\partial p}{\partial x} + \frac{1}{2}\alpha F_2 \left(\frac{\partial p}{\partial x}\right)^3 \right] + U\left\{ 1 - \frac{4y - \alpha F_3 \left(\partial p/\partial x\right)^2}{4H + \alpha H^3 \left(\partial p/\partial x\right)^2} \right\} \tag{6.3.2}$$

where the functions F_1, F_2 and F_3 are described by

$$F_1 = 2y^2 - 2Hy, \tag{6.3.3a}$$

$$F_2 = 2y^2 - 4Hy^3 + 3H^2 y^2 - H^3 y, \tag{6.3.3b}$$

$$F_3 = 6Hy^2 - 4y^3 - 3H^2 y. \tag{6.3.3c}$$

Integrating the continuity equation (6.2.2) across the film height under the relevant boundary conditions (6.2.5a) and (6.2.5b) the modified Reynolds equation is obtained as

$$\frac{\partial}{\partial x}\left[H^3 \frac{\partial p}{\partial x} + \frac{3}{20}\alpha H^5 \left(\frac{\partial p}{\partial x}\right)^3 \right] = 6\mu U \frac{\partial H}{\partial t} \tag{6.3.4}$$

6.4 Stochastic Reynolds equation

Let $f(h_s)$ be the probability density function of the stochastic film thickness h_s. Taking the average of the equation (6.3.4) with respect to $f(h_s)$ we obtain

$$\frac{\partial}{\partial x}\left[E(H^3)\left(\frac{\partial E(p)}{\partial x}\right)+\frac{3}{20}\alpha E(H^5)\left(\frac{\partial E(p)}{\partial x}\right)^3\right]=6\mu U\frac{\partial H}{\partial t}, \tag{6.4.1}$$

where the expectancy operator $E(\bullet)$ is defined by

$$E(\bullet)=\int_{-\infty}^{\infty}(\bullet)f(h_s)dh_s. \tag{6.4.2}$$

In accordance with the Christensen (1969-70), it is assumed that

$$f(h_s)=\begin{cases}\dfrac{35}{32c^7}(c^2-h_s^2)^3. & -c<h_s<c\\ 0 & \text{elsewhere}\end{cases} \tag{6.4.3}$$

Where $\sigma=c/3$ is the standard deviation.

According to the Christensen (1970) stochastic theory for the hydrodynamic lubrication of rough surfaces, the analysis is done for two types of one- dimensional surface roughness patterns viz. one-dimensional longitudinal surface roughness pattern and transverse roughness pattern.

One- dimensional longitudinal roughness pattern

In this case the roughness is assumed to have the form of long, narrow ridges and valleys running in the *x*- direction. The film thickness therefore described by a function of the form

$$H = h(x, y) + h_s(y, \xi)$$

(6.4.4)

and stochastic modified Reynolds equation takes the form

$$\frac{\partial}{\partial x}\left[E(H^3)\left(\frac{\partial E(p)}{\partial x}\right) + \frac{3}{20}\alpha E(H^5)\left(\frac{\partial E(p)}{\partial x}\right)^3 \right] = 6\mu U \frac{\partial E(H)}{\partial t} \tag{6.4.5}$$

One dimensional Transverse roughness pattern

In this type the roughness it is assumed to have the roughness in the form of long narrow ridges and furrows running in the direction perpendicular to the direction of sliding i.e.in the y-direction. The film thickness is therefore described by the function of the form

$$H = h(x, y) + h_s(x, \xi) \tag{6.4.6}$$

and stochastic modified Reynolds equation takes the form

$$\left.\begin{aligned} \frac{\partial}{\partial x}\left[\frac{1}{E\left(1/H^3\right)}\left(\frac{\partial E(p)}{\partial x}\right) + \frac{3}{20}\alpha \frac{1}{E\left(1/H^5\right)}\left(\frac{\partial E(p)}{\partial x}\right)^3 \right] \\ = 6\mu U \frac{\partial}{\partial x}\frac{E\left(1/H^2\right)}{E\left(1/H^3\right)} \end{aligned}\right\} \tag{6.4.7}$$

Equations (6.4.5) and (6.4.7) together can be defined as

$$\frac{\partial}{\partial x}\left[G_1(H, c)\left(\frac{\partial E(p)}{\partial x}\right) + \frac{3}{20}\alpha G_2(H, c)\left(\frac{\partial E(p)}{\partial x}\right)^3 \right] = 6\mu U \frac{\partial M}{\partial x} \tag{6.4.8}$$

where

$$G(H,c)=\begin{cases} E(H). & \text{for longitudinal roughness} \\ \left[E\left(\frac{1}{H}\right)\right]^{-1} & \text{for transverse roughness} \end{cases} \tag{6.4.9a}$$

$$E(H)=\frac{35}{32c^7}\int_{-c}^{c} H(c^2-h_s^2)^3\,dh_s\ , \tag{6.4.9b}$$

$$E\left(\frac{1}{H}\right)=\frac{35}{32c^7}\int_{-c}^{c}\frac{(c^2-h_s^2)^3}{H}\,dh_s\ . \tag{6.4.9c}$$

$$M=\begin{cases} E(H) & \text{for longitudinal roughness} \\ \dfrac{E\left(1/H^2\right)}{E\left(1/H^3\right)} & \text{for transeverse roughness} \end{cases} \tag{6.4.9d}$$

using the non-dimensional variables and parametersss

$$\left.\begin{aligned} &\beta=\frac{\alpha\mu^2U^2}{h_2^2},\ x^*=\frac{x}{L};\ r=\frac{h_1}{h_2};\ H^*=h^*+h_s^*; \\ &h^*=(r-1)(1-x^*)+1;\quad p^*=\frac{E(p)h_2^2}{\mu UL};\ C=c/h_0 \end{aligned}\right\} \tag{6.4.10}$$

where r denotes the inlet-outlet film height ratio and β describes the non-dimensional non-linear parameter. The non-dimensional Reynolds equation and pressure boundary conditions can be defined as

$$\frac{\partial}{\partial x^*}\left[G_1^*\left(H^*,C\right)\left(\frac{\partial p^*}{\partial x^*}\right)+\frac{3}{20}\beta G_2^*\left(H^*,C\right)\left(\frac{\partial p^*}{\partial x^*}\right)^3\right]=6\frac{\partial M^*}{\partial x^*}, \tag{6.4.11}$$

$$p^*=0 \ \text{ at } \ x^*=0 \ \text{ and } \ p^*=0 \ \text{ at } \ x^*=1 \tag{6.4.12}$$

Since equation (6.4.11) is highly non-linear ordinary differential equation which can be solved by applying the small perturbation method

$$p^* = p_0^* + \beta p_1^*. \tag{6.4.13}$$

Substituting (6.4.13) in to (6.4.11) governing equations for p_0^* and p_1^* can be obtained as

$$\frac{\partial}{\partial x^*}\left\{ G_1^*\left(H^*, C\right)\frac{\partial p_0^*}{\partial x^*}\right\} = 6\frac{\partial M^*}{\partial x^*} \tag{6.4.14}$$

$$\frac{\partial}{\partial x^*}\left\{ G_1^*\left(H^*, C\right)\frac{\partial p_1^*}{\partial x^*} + \frac{3}{20}G_2^*\left(H^*, C\right)\left(\frac{\partial p_0^*}{\partial x^*}\right)^3\right\} = 0 \tag{6.4.15}$$

Integrating equations (6.4.14) and (6.4.15) and using boundary conditions (6.4.12) expression for pressure is obtained as

$$p_0^* = \frac{6}{\phi_{B1}}\left(\phi_A\phi_{B1} - \phi_B\phi_{A1}\right),$$

$$p_1^* = \frac{3\beta}{20\phi_{B1}}\left(\phi_B\phi_{C1} - \phi_C\phi_{B1}\right) \quad \text{and}$$

$$p^* = \frac{6}{\phi_{B1}}\left\{\left(\phi_A.\phi_{B1} - \phi_B\phi_{A1}\right) + \frac{\beta}{40}\left(.\phi_B\phi_{C1} - \phi_C.\phi_{B1}\right)\right\} \tag{6.4.16}$$

where

$$\phi_A(x^*) = \int_0^{x^*}\frac{M^*}{G_1^*\left(H^*, C\right)}dx^*, \tag{6.4.17}$$

$$\phi_B(x^*) = \int_0^{x^*}\frac{1}{G_1^*\left(H^*, C\right)}dx^*, \tag{6.4.18}$$

$$\phi_C\left(x^*\right) = \int_0^{x^*}\frac{G_2^*\left(H^*, C\right)}{G_1^*\left(H^*, C\right)}\left(\frac{6\left(M^*\phi_{B1} - \phi_{A1}\right)}{G_1^*\left(H^*, C\right)\phi_{B1}}\right)dx^* \text{ and} \tag{6.4.19}$$

$$\phi_{A1} = \phi_A\left(x^* = 1\right),\ \phi_{B1} = \phi_B\left(x^* = 1\right),\ \text{and } \phi_{C1} = \phi_C\left(x^* = 1\right).$$

The load carrying capacity can be obtained by integrating film pressure over the film region.

$$W = \int_0^L p^* dx^* \tag{6.4.20}$$

which is in the non-dimensional form

$$W^* = \frac{Wh_2^2}{\mu UL^2} = \int_0^1 p^* dx^*$$

$$W^* = \frac{6}{\phi_{B1}}\left\{\left(\xi_A.\phi_{B1} - \phi_{A1}.\xi_B\right) + \frac{1}{40}\beta\left(\xi_B.\phi_{C1} - \xi_C.\phi_{B1}\right)\right\} \tag{6.4.21}$$

where

$$\xi_A = \int_0^1 \int_0^{x^*} \frac{M^*}{G_1^*\left(H^*, C\right)} dx^*,$$

$$\xi_B = \int_0^1 \int_0^{x^*} \frac{1}{G_1^*\left(H^*, C\right)} dx^*,$$

$$\xi_C = \int_0^1 \int_0^{x^*} \frac{G_2^*\left(H^*, C\right)}{G_1^*\left(H^*, C\right)}\left(\frac{6\left(M^*\phi_{B1} - \phi_{A1}\right)}{G_1^*\left(H^*, C\right)\phi_{B1}}\right)^3 dx^*.$$

The frictional force can be obtained by integrating the shear stress acting upon the sliding surface

$$f_f = \int_{x=0}^{L} \left(\tau_{xz}\right)_{at\ z=0} dx \tag{6.4.22}$$

which is in the non-dimensional form

$$F = \frac{f_f h_2}{\mu UL} = \int_{x^*=0}^{1} \left\{\frac{1}{H^*} + \frac{1}{2}H^*\frac{\partial p^*}{\partial x^*} - \frac{\beta}{16}H^*\left(\frac{\partial p^*}{\partial x^*}\right)^2\right\} dx^* \tag{6.4.23}$$

The non-dimensional coefficient of a friction is calculated by

$$C_f = F / W^* \tag{6.4.24}$$

6.5 Results and discussion

The surface roughness effects on static characteristics of plane slider bearing are analyzed by applying small perturbation method. In this study the bearing characteristics are presented with inlet-outlet film ratio.

Figure 6.2 depicts the variation of non-dimensional pressure p^* with x^* for different values of non-linear factor of the lubricant β It is observed that, for both types of roughness patterns there exists critical value of x^* for which pressure is maximum. It is also observed that p^* is more accentuated for transverse roughness pattern than the longitudinal roughness pattern. The variation of non-dimensional pressure p^* with x^* for different values of *C*, for both pseudoplastic and dilatant fluids are as shown in Figures 6.3 and 6.4 respectively. It is clear from these figures that, as the roughness parameter increases pressure also increase for both dilatant and pseudoplastic lubricants. Further, more pressure exerted for transverse roughness pattern.

Figure 6.5 shows the variation of non-dimensional load carrying capacity W^* with *r* for different values of β with $C = 0.2$. It is observed that, load carrying capacity is more for dilatant lubricants as compared with the pseudoplastic lubricants. Further, it is observed that the effect of transverse roughness is to increase the load carrying capacity for all values of β up to certain values of *r* ($r \approx 2.2$) thereafter decreases. Whereas, the presence of longitudinal roughness pattern on the bearing surface causes a decrease in load carrying capacity as compared to the transverse pattern. Thus the surface roughness effects are strongly dependent on surface texture. The variations of non-dimensional load

carrying capacity W^* with r for different values of C with $\beta = 0.08$ and $\beta = -0.08$ are depicted in Figures 6.6 and 6.7 respectively. It is observed that, as the values of C increase the load carrying capacity increases, in case of transverse roughness pattern up to certain values of r thereafter, decreases but reverse trend is observed in the case of longitudinal roughness pattern. Further, it is also observed that, load carrying capacity is more for dilatant lubricants as compared with pseudoplastic lubricants.

The variation of non-dimensional frictional force F with the inlet-outlet height ratio r for different values of β is depicted in Figure 6. 8. It is clear from the figure that as r increases, F decreases for dilatant lubricants are more pronounced than pseudoplastic fluids. Figures 6.9 and 6.10 depicts the variation of frictional force, F with the inlet-outlet height ratio r for different values of C with $\beta = 0.08$ and $\beta = -0.08$ as r values increases, frictional force F decreases. Further, it is also observed that as roughness parameter C increases frictional force also increases. If $C = 0$, the results are in agreement with smooth case studied by Lin *at al.* (2016). Also it is noted that, the dilatant lubricants show larger frictional force as compared with pseudoplastic lubricants.

Figure 6.11 shows the variation of coefficient of friction C_f with r for different values of β with it is observed that C_f tends to decrease as r increases and as β values increases C_f also increases. The variation of coefficient of friction C_f with r for different values of C with $\beta = 0.08$ and $\beta = -0.08$ is depicted in figures 6.12 and 6.13. It is observed that, the dilatant lubricants show less coefficient of friction as compared to pseudoplastic lubricants. Further, it is also observed that, transverse roughness pattern shows less coefficient of friction.

6.6 Conclusions

In the present chapter the effect of surface roughness on the static characteristics of inclined plane slider bearing lubricated with non-Newtonian Rabinowitsch fluid is presented. To obtain steady characteristics of a bearing, modified Reynolds equations are derived and solved by using small perturbation method. The results are in well agreement with that of smooth case ($C \to 0$) studied by Lin *at al*. (2016). Based on the results, so obtained, the following conclusions have been drawn.

1. Static characteristics are functions of roughness parameter *C*, as well as non-linear factor of the lubricant β .
2. Steady state pressure and load carrying capacity increases significantly for the dilatant lubricants as compared with the pseudoplastic lubricants.
3. The steady state load carrying capacity increases with *r* up to $r \approx 2.2$ and decreases thereafter while coefficient of friction decreases with *r* increases.
4. Coefficient of friction is lesser for dilatant lubricants as compared to the pseudoplastic lubricants for both type of roughness patterns, but frictional force is larger for dilatant lubricants as compared to the pseudoplastic lubricants.

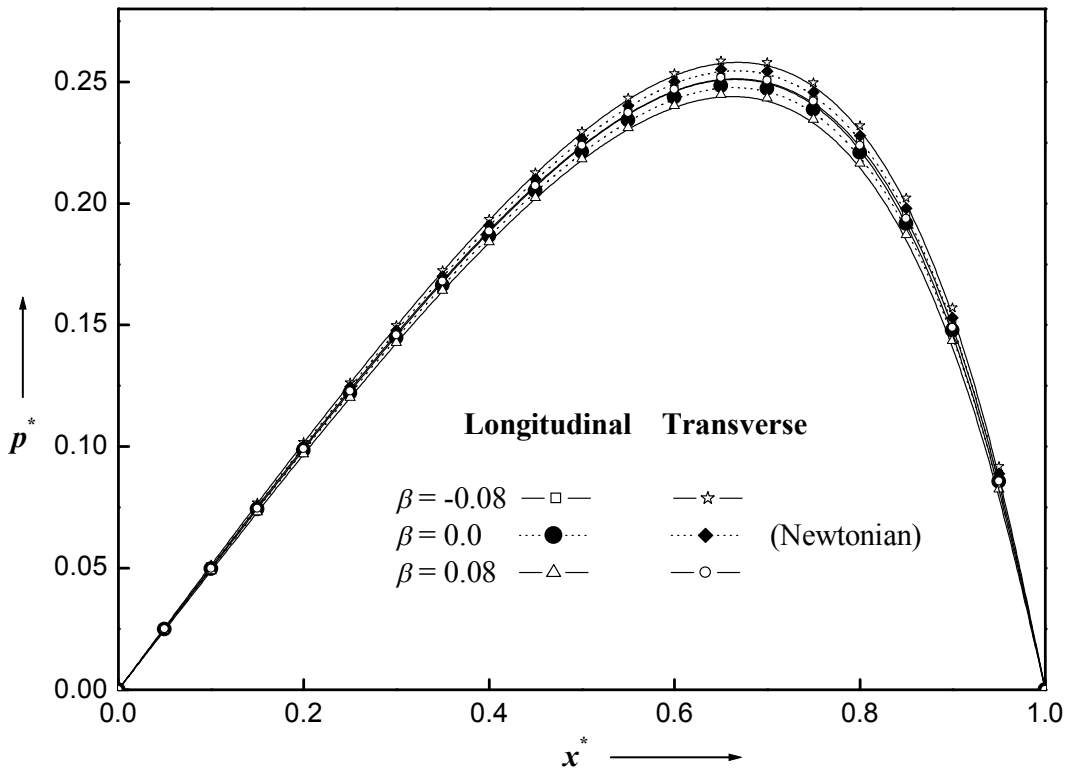

Figure 6.2 Variation of non-dimensional pressure p^* verses x^* for different values of β with $r = 2$ and $C = 0.2$.

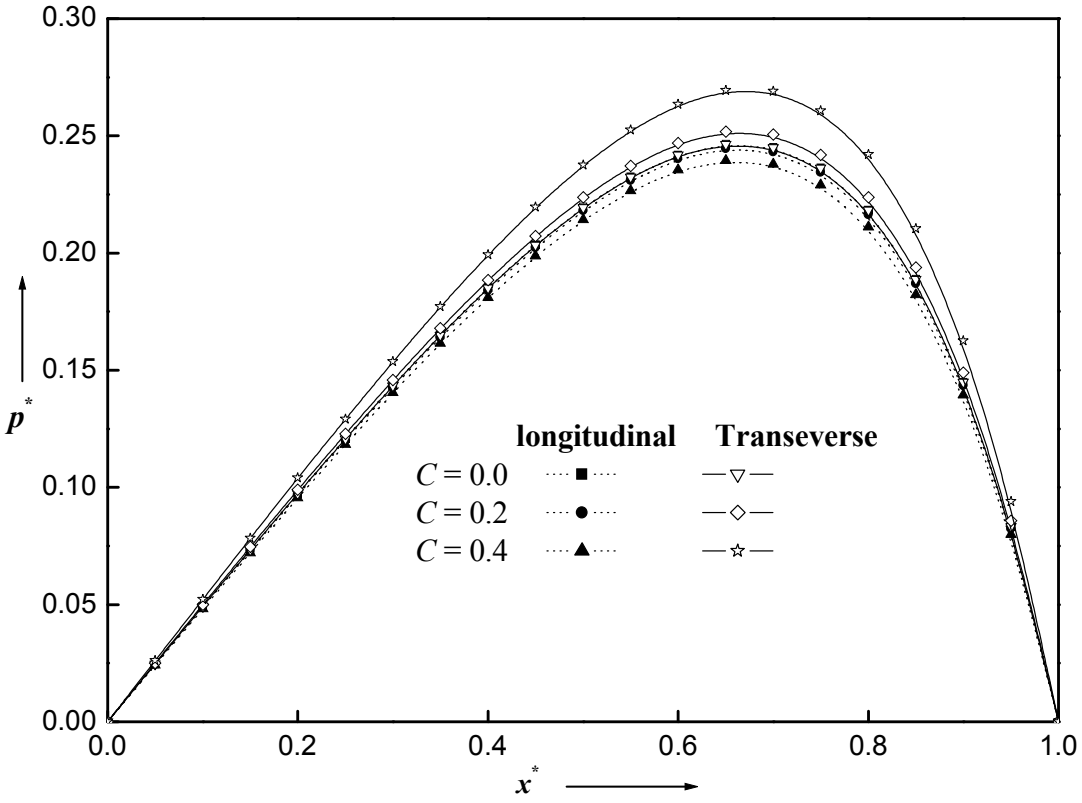

Figure 6.3 Variation of non-dimensional pressure p^* with x^* for different values of C with $r = 2$ and $\beta = 0.08$.

SS

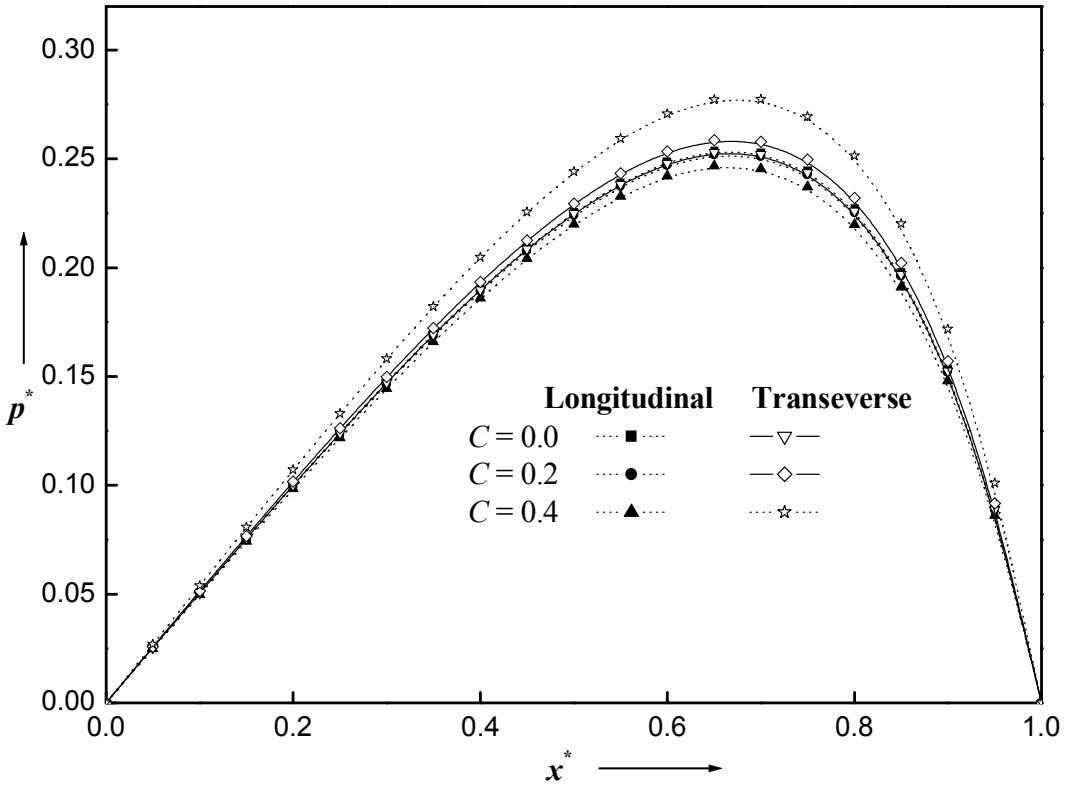

Figure 6.4 Variation of non-dimensional pressure p^* with x^* for different values of C with $r = 2$ and $\beta = -0.08$.

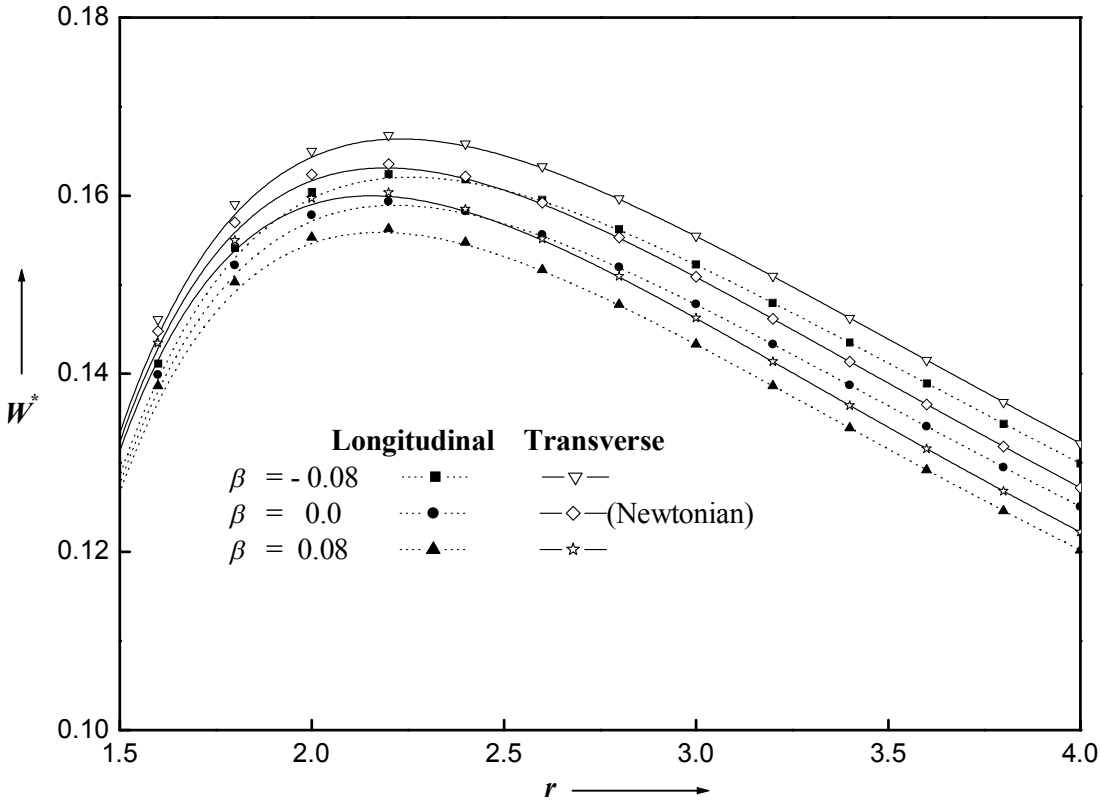

Figure 6. 5 Variation of non-dimensional load carrying capacity W^* with r for different values of β with $C = 0.2$.

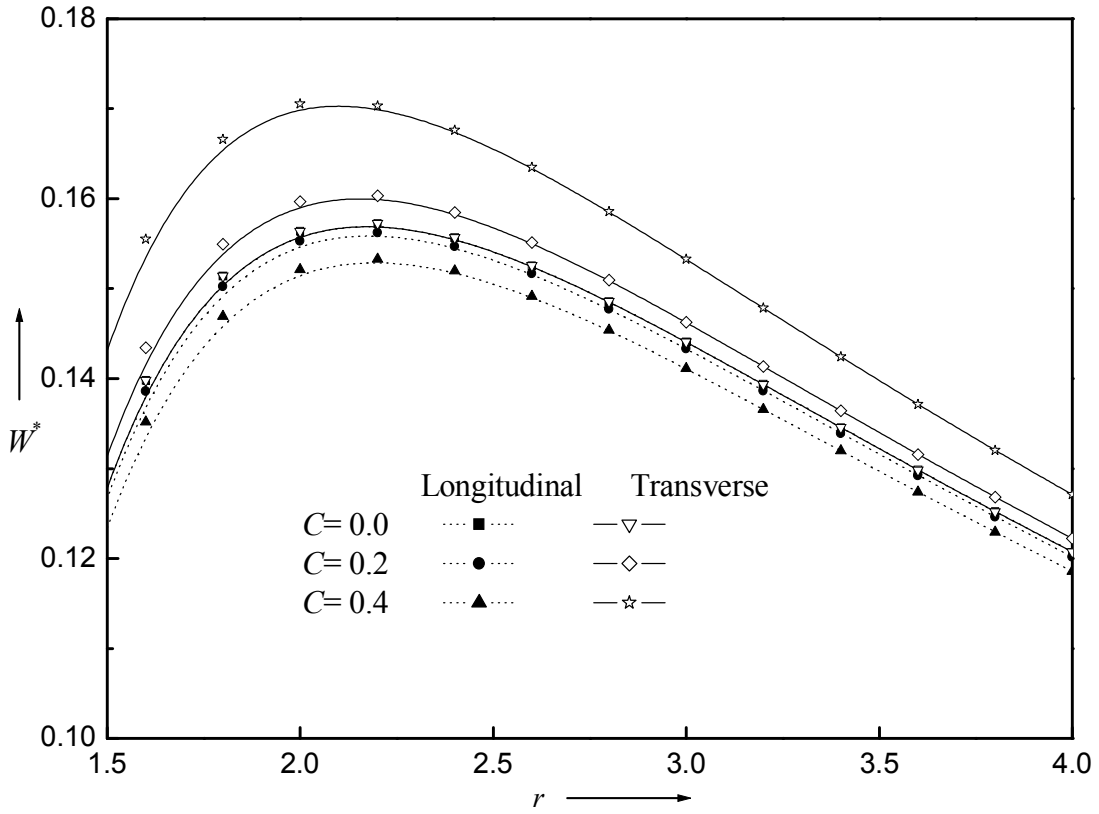

Figure 6.6 Variation of non-dimensional load carrying capacity W^* with r for different values of C with $\beta = 0.08$.

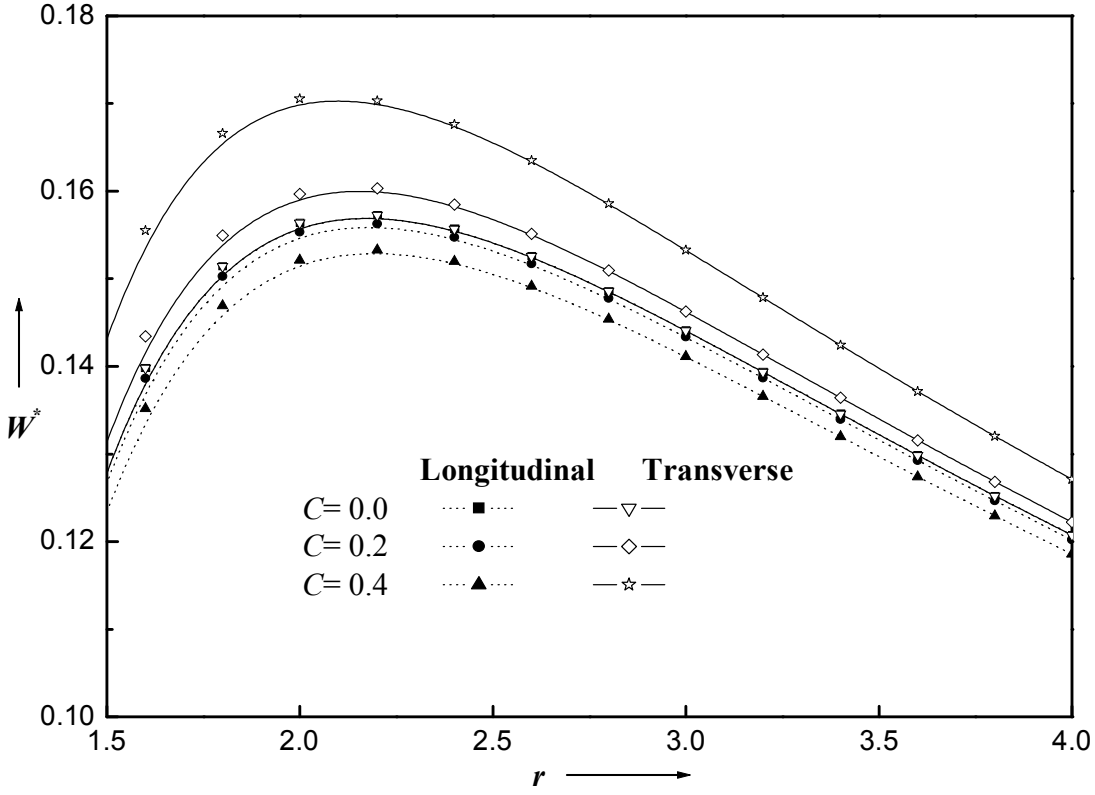

Figure 6.7 Variation of non-dimensional load carrying capacity W^* with r for different values of C with. $\beta = -0.08$

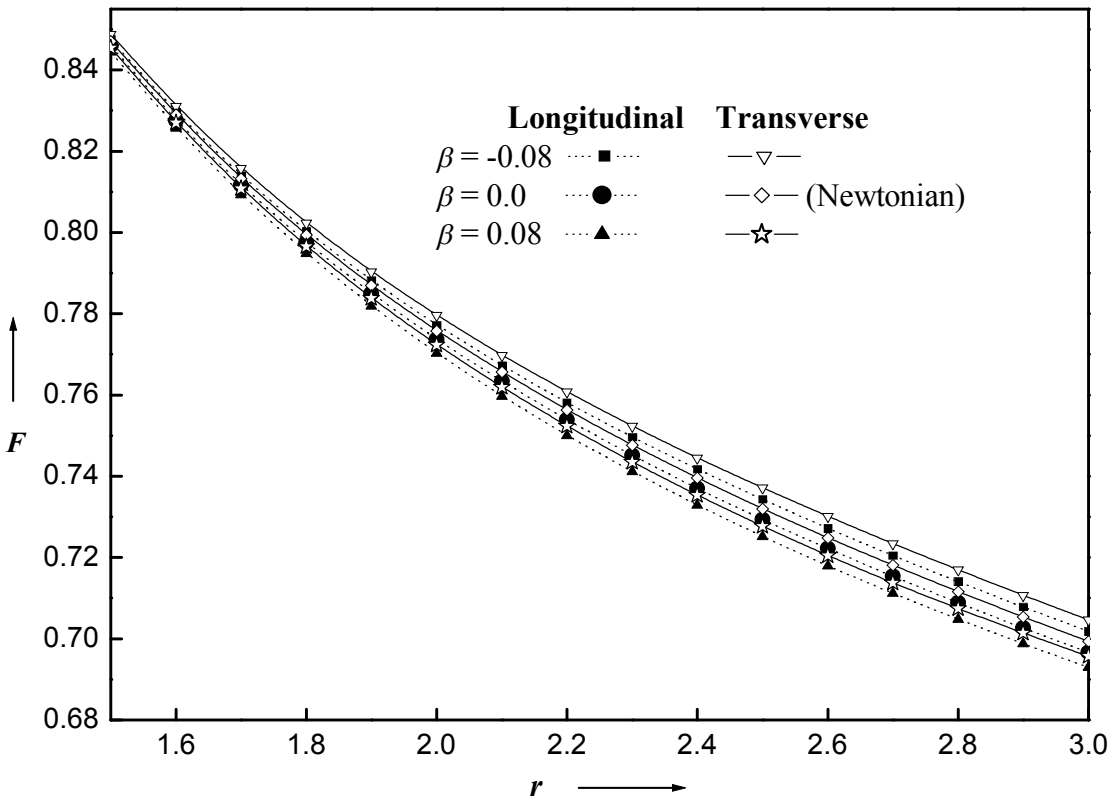

Figure 6.8 Frictional forces F verses the inlet-outlet height ratio r for different values of β

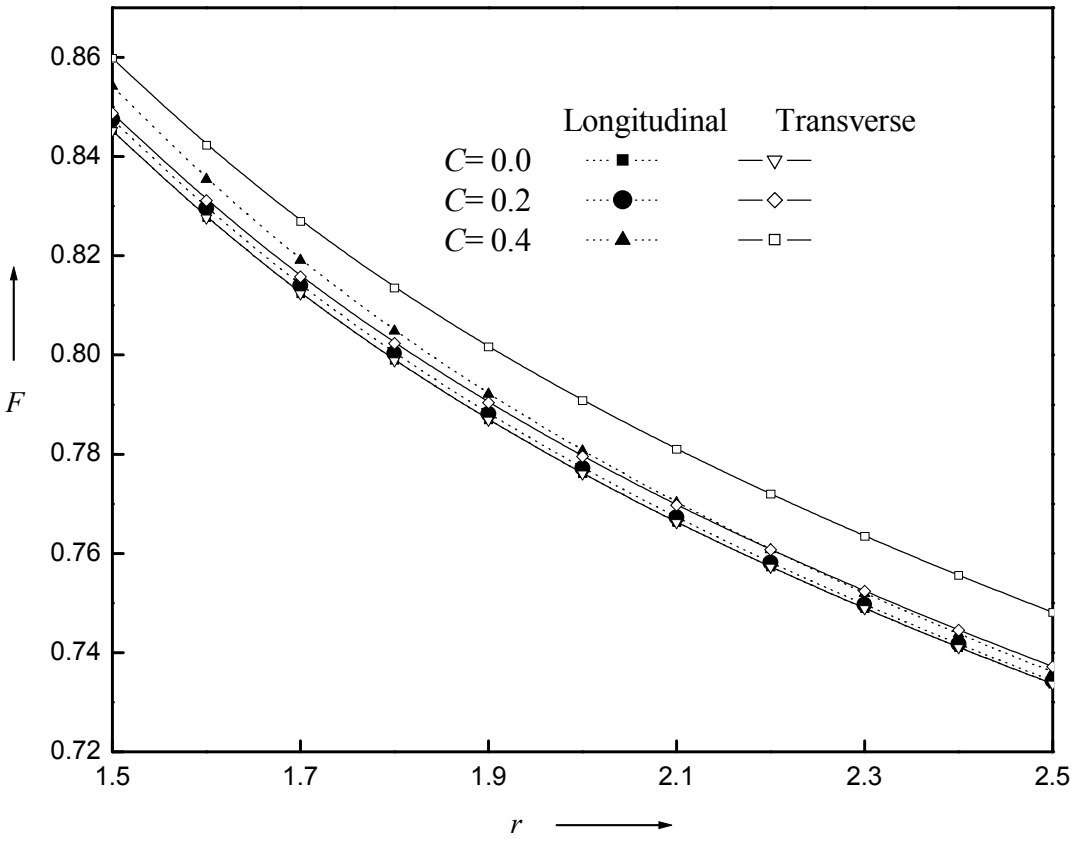

Figure 6.9 Frictional forces F verses the inlet-outlet height ratio r for different C with $\beta = -0.08$

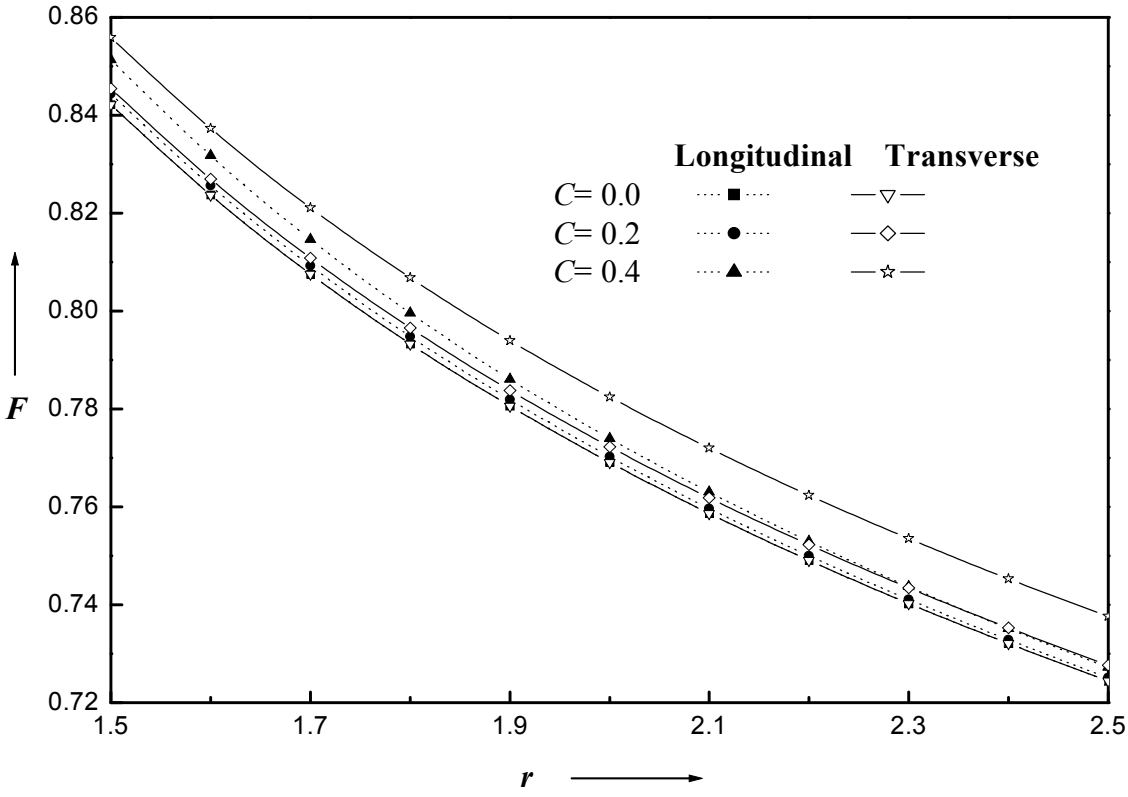

Figure 6. 10 Frictional forces F verses the inlet-outlet height ratio r for different C with $\beta = 0.08$

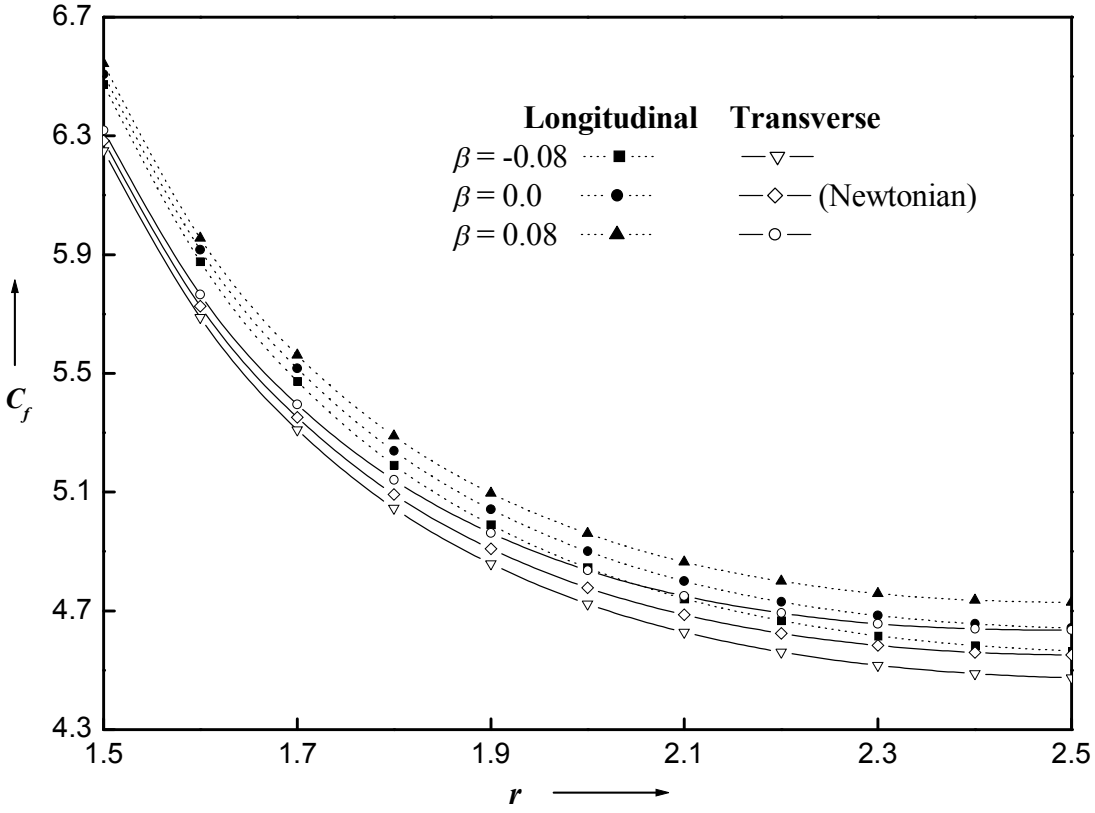

Figure 6.11 Variation of coefficient of friction C_f verses the inlet-outlet height ratio r for different values of β with $C = 0.2$.

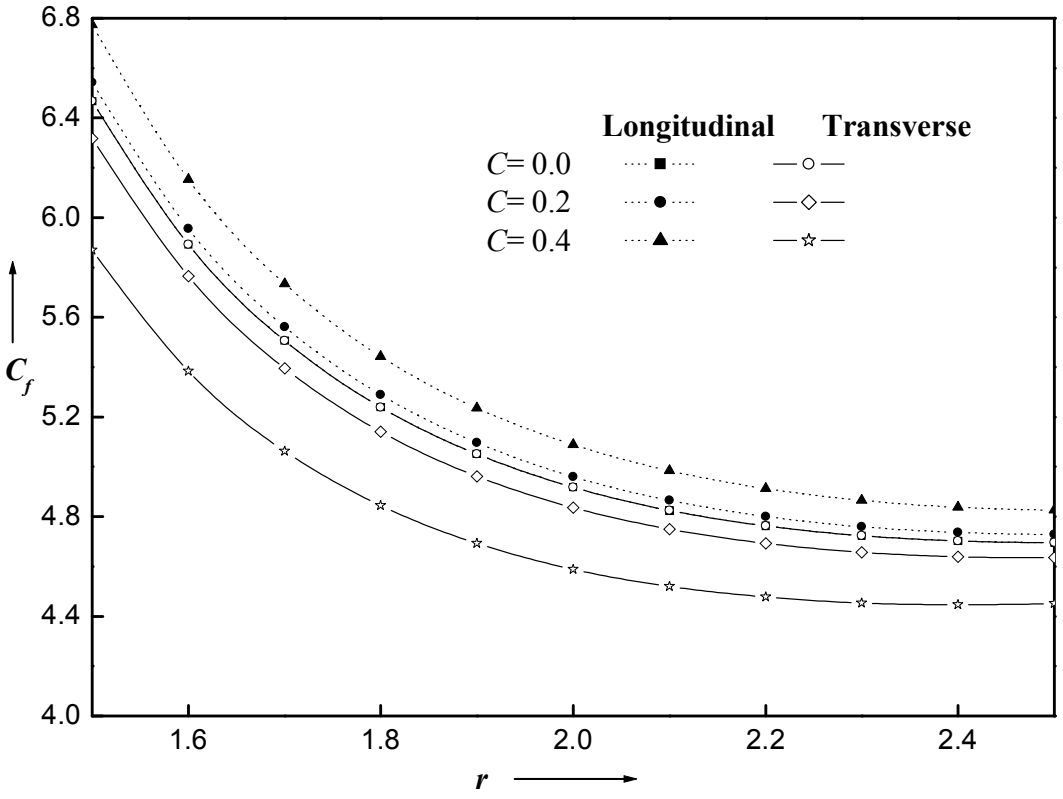

Figure 6.12 Variation of coefficient of friction C_f verses the inlet-outlet height ratio r for different values of C with $\beta = 0.08$

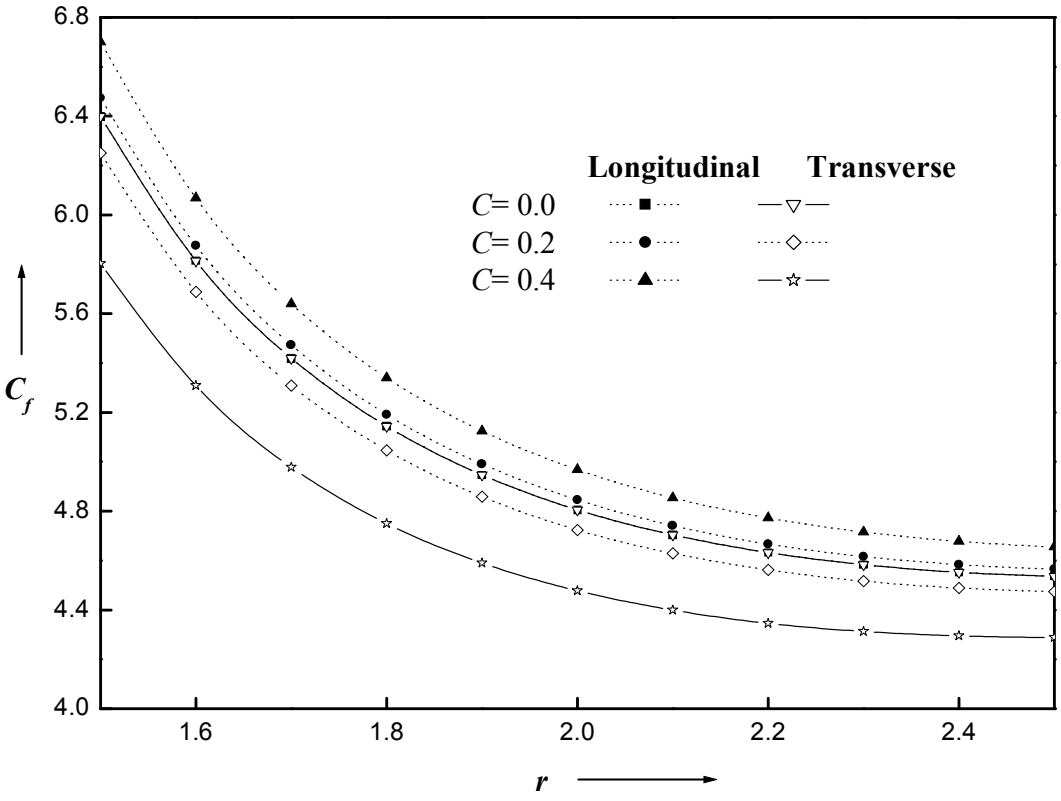

Figure 6.13 Variation of coefficient of friction C_f verses the inlet-outlet height ratio r for different values of C with $\beta = -0.08$